To appear in International Journal of Impact Engineering

Springback of circular clamped armor steel plates subjected to spherical air-blast loading

A.Neuberger[a*], S.Peles[b], D.Rittel[c]

[a] *AN Armor Solutions Ltd., POB 513 Nordiya,42954, Israel.*

[b] *IMI, Central Laboratory Division, Ramat Hasharon, POB 1044, Israel.*

[c] *Technion, Israel Institute of Technology, Faculty of Mechanical Engineering, 3200 Haifa, Israel.*

Abstract

The development of protective elements (plates) that are impulsively loaded requires comprehensive experiments in which the transient dynamic and residual deflections are measured. Whereas the residual plastic deflections are easily measured upon completion of the experiment, transient deflection measurements involve more elaborate setups. Relying on the residual deflection only can be misleading when one tries to assess the peak transient deflection which poses a real hazard to the protected subject. In this study, the peak transient and the residual deflections are compared for a clamped circular armor steel plate subjected to large close-range spherical air-blast loading. The difference between the maximal transient and the residual plastic deflection is addressed here as the elastic springback.

We report experimental results from a series of controlled explosion experiments and finite elements computer calculations. A quantitative relation is presented between the springback magnitude and the distance to the explosive source. In addition, the springback is also observed to reach a maximum which marks a transition from an essentially elastic to plastically dominated deformation.

[*] *Corresponding author: navidov@gmail.com*

***Keywords**: springback, blast, dynamic response, scaling, circular plate.*

Nomenclature

D	plate diameter
D*	Cowper Symonds material constant
E_p	hardening modulus
I	impulse
P	pressure
P_i	incident pressure
P_r	reflected pressure
q	Cowper Symonds material constant
R	distance from center of charge (standoff)
R_c	critical distance from charge (inflexion distance)
S	scaling factor
t	plate thickness
W	charge weight
Δ_δ	dynamic springback
δ_r	residual mid-point deflection
δ_t	maximal mid-point transient deflection
ε	The relative difference in experimental and numerical residual deflections
$\dot{\varepsilon}$	equivalent strain rate
θ	angle of incidence
σ_d	dynamic yield stress
σ_y	Static yield stress
τ	time

1. Introduction

The literature on the dynamic plastic behavior of blast loaded plates is quite rich, and various references of theoretical, experimental and numerical nature have been reported. References [1] to [18] span the field from different points of view, starting from the shape

of the plate (square, circular or shell), boundary conditions (clamped or simply supported), type of the impulsive load (variety of blast pulses, uniform or localized) and finally, the nature or mode of the deformation or failure. Different failure modes were first defined by Menkes and Opat [19] for the case of impulsively loaded clamped beams. According to their classification mode I was for large inelastic deformation, mode II for tearing at the support, and mode III for shear failure at the support. These failure modes were also adopted for blast loaded circular plates, and further subdivisions were observed and defined by other authors. However, the previously mentioned studies focused mainly on the *residual* deformation or failure of the plate, while the elastically driven change of shape of the plate upon unloading, i.e. *springback*, was not emphasized.

Springback is traditionally associated with sheet metal forming, where it refers to the elastically driven shape change of a part upon unloading after plastic forming. Some recent works addressed the problem of springback prediction in the forming of high strength materials, and focused on the control [20] and computational analysis [21] methods to ensure reduction of the springback effect. However, the issue of interest here is that of structural springback in the context of explosive loading. Schleyer et al. [22] presented a methodology to provide adequate predictions of the dynamic large-deflection response of mild steel plates subjected to uniform pulse pressure loads. The plate behavior was dominated by membrane effects leading to substantial springback that was predicted with reasonably good success.

When designing protective elements, the consideration of the sole final residual deformation can be misleading, for example, when a sensitive device is to be placed behind a protective wall. Here, one should take into account the maximal dynamic bulging that can destroy the protected subject, so that the distance from the protective element is critical from the point of view of survivability. In other words, one would like to have an accurate estimate of the maximum deflection which amounts to the sum of the residual and springback deflections. This is the central theme of this work.

The generic problem is as follows: a peripherally clamped circular RHA armor steel plate is subjected to symmetric spherical TNT air-blast loading. This causes dynamic bulging of the plate's mid-point (center) up to a maximal transient deflection, followed by damped elastic oscillations leading to the residual deformation pattern. This paper

investigates the relation between the maximal transient and residual deflections. The variable parameters of the problem are the plate thickness and standoff distance from the explosive charge.

The results presented here are partly based on tests reported in our previous paper [23] where we presented experiments at different reduced scales of the generic problem discussed here. The main focus in [23] was on the *maximal transient elastic deflection*, while the overall physical picture is completed here by addressing *residual plastic deformations*. The current study combines previous experimental and new numerical results. Indeed, whereas the experimental results were reported in [23], the numerical results had to be recalculated since the original data focused on the first stage of the process, i.e. the first peak, while the current study addresses specifically long term effects, namely residual deformations.

The numerical model investigated here is a peripherally clamped circular RHA steel plate, with a diameter of 1m and 4 different thicknesses: 10, 15, 20 and 25mm which are standard manufactured thicknesses. The plate is subjected to the explosion of a 15Kg spherical TNT charge, at different standoff distances, starting from 1m down to 0.275m. In parallel to the numerical calculations, the experiments were carried out on a 20mm thick plate, with a 3.75Kg TNT charge at 0.2m standoff distance, and a 8.75Kg TNT charge at 0.13m and 0.2m standoff distances, respectively. Note that the transient deflection experimental results where reported in [23], whereas the residual deflection data is reported here for the first time.

The paper is organized as follows: section 2 presents the numerical simulations, and section 3 describes the experimental setup. Section 4 presents experimental and numerical results. Finally, section 5 discusses the key points of the study, followed by concluding remarks.

2. Numerical simulations

The numerical simulations procedure has been described in detail in [23], and will only briefly be outlined here. Simulations were carried out using LS-DYNA finite element code [24]. A pure Lagrangian approach was adopted, together with a simplified engineering blast model of a spherical charge to reduce the calculation time.

2.1. Simplified blast function

The 'load-blast' function implemented in LS-DYNA is based on an implementation by Randors-Pehrson and Bannister (1997) of the empirical blast loading functions by Kingery and Bulmash [25] that were implemented in the US Army technical manual ConWep code [26].

The blast loading equation is stated as follows

$$P(\tau) = P_r \cdot \cos^2\theta + P_i \cdot \left(1 + \cos^2\theta - 2\cos\theta\right) \tag{1}$$

where θ is the angle of incidence, defined by the tangent to the wave front and the target's surface, P_r is the reflected pressure, and P_i is the incident pressure. This blast function can be used for the following two cases: free air detonation of a spherical charge, and ground surface detonation of a hemispherical charge. To calculate the pressure over certain predefined group of surfaces related to the geometry of the analyzed structure, the model uses the following inputs: equivalent weight of TNT explosive, the spatial coordinate of the detonation point, and the type of blast (spherical or hemispherical). The actual impulse, I, corresponding to the charge's weight and distance to the target, can be derived from the ConWep code [26]. For example, considering the problem analyzed here where the spherical TNT charge's weight is W=15Kg, and the distance from the target is R=1m, the peak incident overpressure is 5,017kPa, the normally reflected pressure 41,430kPa, the impulses are I(incident)=316kPa·msec, and I(reflected)=4,147 kPa·msec. By bringing the charge closer to the target, R=0.275m is the closest standoff that we have numerically investigated with regard to the 15KgTNT, the peak incident overpressure becomes 27,980kPa, the normally reflected pressure 328,800kPa, the incident impulse is I(incident)=1532kPa·msec, and the reflected impulse

I(reflected)= 43,690kPa·msec (note that for the closer standoff the model may be not so accurate in producing the waveform).

2.2. RHA steel plate material behavior

The circular steel plate is represented by a finite element mesh created by FEM-PATRAN preprocessor software [27]. Using symmetry the problem calculation time can be reduced, so that only a quarter of the circular plate and the clamping rings were modeled with the appropriate boundary conditions applied along the symmetry planes as shown in figure 1. The entire model was constructed from constant stress hexagonal solid elements with one integration point.

The plate material (RHA steel) was modeled as a rate-sensitive elastic-plastic bilinear material obeying Von Mises yield criterion. Generally, this material model is suitable to model isotropic and kinematic hardening plasticity. Strain rate effects are accounted for based on the Cowper-Symonds model [28] in which:

$$\frac{\sigma_d}{\sigma_y} = 1 + \left(\frac{\dot{\varepsilon}}{D^*} \right)^{1/q} \tag{2}$$

where σ_d is the dynamic yield stress, σ_y is the static yield stress, $\dot{\varepsilon}$ is the equivalent strain rate, D^* and q are material constants. The following parameters were used here[†]: for the bilinear stress strain curve the static yield stress σ_y=1200 MPa and strain hardening modulus E_p=6.5GPa. For the Cowper-Symonds model, coefficients D^*=300s^{-1} and q=5.

While this model may not be the most sophisticated to analyze both transient and residual deflections, in the sense that unloading does not take into account any Bauschinger effect, it is felt that it is certainly sufficient to properly determine the principal trends of the problem, with the advantage of its great simplicity.

[†] We found this set of parameters to fit quite well with the experimental results. In this work we chose to model the RHA steel according to the model used in [8] that uses the set of parameters D^*=40s^{-1} and q=5 for mild steel. However, we kept q=5 and modified D^*=300s^{-1} as an ad-hoc value to lower the strain-rate sensitivity as expected from a high strength steel as compared to mild steel. Let us remind that the strain rates developed in such a problem are of the order of 10^2 s^{-1} [23].

The response of the plate was calculated over a relatively long period of time (30 ms), such as to capture the peak transient deflection as well as the stabilized response, i.e. the residual deflection.

3. Test setup

The experimental setup is shown in figure 2. This is basically the setup used in [23], which will only be briefly described here. The target plate is clamped with two thick armor steel rings, tightened together with bolts and clamps. The thick plate facing the charge has a hole with inclined side walls to reduce reflection of the blast wave to the tested plate as shown schematically in figure 3. The measured parameter is the residual deflection, δ_r, and the maximal transient deflection, δ_t. The latter was measured at the center of the plate using the a comb-like device [23]. The teeth of the comb possess a gradually decreasing height, and when positioned under the dynamically deflecting plate, the long teeth are permanently bent while those that are shorter than the maximum deflection remain intact. Therefore, a direct estimation of the maximum deflection is immediately available after the blast test. Note that the accuracy of the measurement is related to the height difference between the teeth, which is equal to 3mm in our experiments. While the peak deflection was measured "online" using the comb, the residual deflection profile was measured at the end of the experiment. The spherical TNT charges were hanged in air and were ignited from the center of the charge.

4. Experimental validation of the numerical model

The measured maximal dynamic deflection of 20mm RHA steel plate was reported in [23] for different spherical TNT charges. We shall use part of this data with the additional residual experimental results (un-reported) to validate the finite elements new simulations that were recalculated with the Von Mises material model. Table I presents the experimental and numerical results of a 20mm thick RHA steel plate with 1m diameter that is subjected to blast loads of different intensities. The comparison here is for three different cases. The first case (a) corresponds to a relatively small charge, and the

dynamic response is mostly elastic, almost without any residual deflection. By contrast, the other two cases (b and c) are for larger charges from two different close ranges, and the response of the plate is mostly plastic, as evidenced from the noticeable residual deflection.

Table I: Experimental and numerical results of transient and residual deflections*

Case	W (Kg TNT)	R (m)	δ_t / t Experimental	δ_t / t Numerical	δ_r / t Experimental	δ_r / t Numerical	ε**
a	3.75	0.20	2.70 ±0.15	2.62	0.35	0.55	0.57
b	8.75	0.20	5.35 ±0.15	5.41	3.20	3.77	0.16
c	8.75	0.13	8.25 ±0.15	8.15	6.05	5.92	0.02

* Clamped 20mm thickness RHA steel plate, 1m diameter.

** The relative difference in residual deflection is given by: $\varepsilon = \left| \frac{\left(\frac{\delta_r}{t}\right)_{num} - \left(\frac{\delta_r}{t}\right)_{\exp}}{\left(\frac{\delta_r}{t}\right)_{\exp}} \right|$

*** It should also be kept in mind that the material parameters, irrespective of the performance of ConWep for small standoff, were optimized to minimize the error for case (c) which is characterized by a large residual deflection. In doing so, the accuracy of cases (a) and (b) is inevitably smaller since the residual deflection is increasingly smaller. While both the experimental and numerical results have some inherent errors, the physical behavior of the system is nevertheless well represented, and this is the main focus of this work.

Table I shows good agreement between the calculated and measured normalized transient deflections. The calculated and measured residual deflections are closer to each other as the intensity of the charge increases and the standoff distance decreases. As shown in the rightmost column, the relative difference between calculated and measured (reference) residual deflections, ε, is small for cases (b) and (c), and decreases dramatically for case c. However, for case (a), ε is not that small. Here, one should note that case (a) involves a very small residual deflection, as compared to the transient one, so that it is representative of an essentially elastic structural response. In that case,

normalized values of 0.55 or 0.35 are in fact very close to each other, and overall negligible, so that the relatively high value of ε for case a is not deemed to be critical.

Figure 4 presents the finite elements calculations of the dynamic deflection time history for a 8.75kg TNT charge at a distance of 0.2m. The deflection reaches its maximal transient magnitude in less than 2msec and then oscillates for approximately 30msec until it stabilizes to the residual magnitude. Figures 5 and 6 illustrate the transient and residual deflection states, respectively. Figure 5 shows a frame after 1.3msec when the plate almost reaches the maximal transient deflection, while the residual deflection test result of the 20mm plate is presented in Figure 6.

This preliminary phase shows a good agreement between the experimentally measured deflections and those calculated using the finite element model. This verification phase confers reliability to the numerical model, so that the rest of the study is based on the finite elements simulations.

5. Numerical results and disscusion

Table II: The numerical calculations cases

W [Kg TNT]	15
D [m]	1
t [mm]	10, 15, 20, 25
R [m]	0.275, 0.3, 0.325, 0.35, 0.4, 0.5, 0.75, 1

Table II presents the cases that were modeled numerically.

One can now take advantage of the Hopkinson and replica scaling concepts[‡] presented in [23], assuming that material properties are scaling-independent. One should note that this is usually not the case because of manufacturing constraints [23], however, this assumption is made here for the sake of simplicity. Yet, this specific point can be addressed in practical situations, keeping in mind that the variability of the material

[‡] It should be emphasized that scaling is satisfied provided that the deformations remain ductile, the material is rate-insensitive, and no cracking or failure occurs.

properties during scaling may distort the scaled results, however the magnitude of the distortion can be numerically calculated [23]. In other words, we suggest the following methodology: suppose we numerically calculate a scaled down model and a full size prototype with the same material properties. Knowing that the full scale prototype may have different material properties, recalculation is needed to validate the distortion of the result. Finally the calculated distortion will be used as a correction factor when transforming the experimental scaled down model results to the approximation of the full scale prototype results. Table II provides sets of baseline cases from which further scaling can be applied. For example, one might select as a baseline case W=15kg TNT, D=1m, t=20mm and R=0.5m. The charge intensity can be represented by $15S^3$, where S is the geometrical scaling factor. Therefore, selecting S=2, one obtains a new set of parameters for a similar (scaled) problem: W=120Kg TNT, D=2m, t=40mm and R=1m.

The first result concerns the relation between the transient and residual non-dimensional deflections as function of the non-dimensional standoff distance. Figures 7 to 10 present the calculated normalized maximal transient deflection and the residual midpoint deflection versus the normalized distance from the charge. Note that the deflections and distances are normalized in terms of the plate thickness. Furthermore, each graph presents the results for a specific ratio of the plate diameter to thickness. The upper curve presents the peak deflection while the lower curve presents the final residual deflection in terms of "times thickness". Consider for example Figure 7. Selecting the scaling factor S=1, one gets the following parameters for the discussed problem: the charge weight is 15Kg TNT, the plate's thickness is 10mm, and its diameter is 1m. The deflections resulting from the 15Kg TNT charge operated at a distance of 35 thicknesses (0.35m) are, according to Figure 7: maximal normalized transient $\delta_t/t=6$ ($\delta_t=0.06$m), while the residual δ_r/t reaches 4.5 thicknesses ($\delta_r=0.045$m). Likewise, the same graph can be used for a 30Kg TNT charge if all the geometrical parameters are now multiplied by $S=(2)^{1/3}$.

Two characteristic domains are clearly observed, that are delineated by an inflexion point. The first domain, for which there exists a strongly sensitive response to the standoff distance, is followed by a much less sensitive response. Namely, when the standoff distance is greater than the critical inflexion point, the deflection versus standoff

distance exhibits a mild slope that indicates a reduced sensitivity. By contrast, for closer standoff distances, with respect to the critical inflexion point, the deflection response as a function of the standoff exhibits a steep slope, which indicates a sensitive response to the standoff distance. The critical (inflexion) point is noted here as $(R/t)_c$, ,and table III lists the value of $(R/t)_c$ as a function of the plate geometrical characteristics D/t.

Table III: Critical inflexion point and plate geometrical characteristics

$(R/t)\|_c$	D/t
35	100
23	66.67
17.5	50
14	40

Figure 11 shows the relationship between $(R/t)_c$ and D/t, together with the relationship between the transient normalized deflection, $(\delta_t/t)_c$, and D/t. It appears that the simple following linear relationship fits within the range of the numerical results quite well:

$$R_c \approx 0.35\,D \tag{3}$$

where R_c is the distance from center of charge where the inflexion occurs and D is the diameter of the plate. In other words, $(R/t)_c$ divides the plate response into two domains: one for which the plate deflections are quite sensitive to the standoff distance, and the second in which this sensitivity is markedly decreased. It should be noted that while the critical standoff distance is linearly related to the plate's diameter (eqn. [3]), this is not the case for the maximal transient deflection. Here, the relationship can be described by the following approximation:

$$\left(\frac{\delta_t}{t}\right)_c = 0.2042\left(\frac{D}{t}\right)^{0.7337} \quad @ \quad 40 \le \left(\frac{D}{t}\right) \le 100 \tag{4}$$

Here, one should be careful not to extrapolate the obtained results, this point requiring additional work. Yet, the results presented here cover a wide range of cases (based also on the use of scaling), and the approach introduced here can easily be implemented to other geometrical cases, or other materials not covered here.

Another important result is related to the springback of the plate, the latter being the difference between transient and final deflections. Springback is an important issue that ties together the transient and residual deflections, when other parameters are systematically varied. The springback $\Delta_\delta=\delta_t-\delta_r$ is defined as the difference between the peak transient and residual deflections, as illustrated in Figure 4. Figures 12 to 15 show the normalized (Δ_δ/t) springback as a function of the normalized residual deflection for four different diameter to thickness ratios. Considering figure 13 for example, if the scaling factor S=1, this corresponds to a charge weight of 15Kg TNT, plate thickness is 0.015m, and plate diameter of 1m. In this case, the normalized springback magnitude has a maximum point that reaches $\Delta_\delta/t\approx2.75$ (Δ_δ =41.25mm), while the corresponding residual deflection here is only $\delta_r/t\approx1$ plate's thickness (δ_r=15mm).

The dynamic springback varies as a function of the standoff distance, in a strongly nonlinear way, going through a maximum point. Figures 12 to 15 show the relationship between the dynamic springback and the residual deflection, which exhibits a maximum point. Note that, if we relate the normalized residual deflection at the springback's maximum point (figures 12-15) with the inflexion point (figures 7-10), one can observe that the maximum point of the dynamic springback and the inflexion point correspond to the same standoff distance. This observation applies only to a plate with diameter to thickness ratio $D/t\leq70$, while the case D/t=100 is different, as addressed in the sequel. Within the range of analyzed results, the maximum normalized springback is between $2.5\leq\max(\Delta_\delta/t)\leq2.9$, while the normalized residual deflection is between $0.5\leq\delta_r/t\leq1.2$ respectively. Furthermore, the larger maximal normalized springback, $\max(\Delta_\delta/t)$, corresponds to larger diameter to thickness ratio, D/t. Figures 12 to 15 can also be used to assess the dynamic response for a given residual deflection. For example, in figure 12, suppose a measured non-dimensional residual deflection, $\delta_r/t=6$, the corresponding non-dimensional springback will then be $\Delta_\delta/t\approx1$.

Finally, The physical nature of the response, whether it is essentially elastic or plastic, can be ascertained by plotting the residual to transient deflections ratio, δ_r/δ_t, as a function of the normalized standoff distance, R/t, as shown in figure 16. The general response of the plate shows again 2 domains, each corresponding to a relatively constant value of δ_r/δ_t, separated by a clear transition. This transition is observed to be quite abrupt for the thicker plates ($D/t \leq 70$), as compared to the thinner ones. The two domains correspond to a dominant plastic ($\delta_r/\delta_t \rightarrow 1$), or dominant elastic response of the plate ($\delta_r/\delta_t \rightarrow 0$), as illustrated schematically in figure 17.

6. Summary and Conclusions

This work addresses the relationships between maximum transient and residual deflections of blast loaded plates. The investigation is based on numerical simulations that have been validated in a preliminary phase versus experimental results (table I). Throughout this work, the results are presented in a normalized way including the scaling factor, to allow the use of Hopkinson-replica scaling concepts used in our previous work [23]. Note that in order to use the scaling concept, one should ensure invariance of the material properties at all scales. The results are arranged to provide sets of cases that can be derived from the baseline case which is presented as a function of the scaling factor, so that the cases are geometrically proportional, the charge is scaled according to the cube root relation, and the material properties are identical.

A numerical investigation of fully clamped circular RHA steel plate subjected to spherical air blast is reported. The focus of this investigation is on the dynamic springback of the mid-point deflection. Scaling concepts reported in previous papers were implemented in this study. Test results, partly reported in our previous paper, were used to validate the simple bi-linear numerical model used here. The following conclusions can be drawn from the study:

- The relationship between the transient and residual non-dimensional deflections as function of the non-dimensional standoff, show the existence of an inflexion

point. The critical point divides the distance from charge into two characteristic domains. When the distance from the charge is greater than the critical inflexion point, the deflection response shows a reduced sensitivity to the standoff distance, while for closer standoffs the response is very sensitive to distance from charge.

- The critical distance from charge is linearly related to the plate's diameter, (eqn. [3]). For the problem studied here ($15S^3$ Kg TNT), this distance is equal to 0.35 times the plate's diameter. Note that this relationship is scale-independent.
- By contrast, the amplitude of the effect is a nonlinear function of the plate's diameter (eqn. [4]).
- The dynamic springback as a function of standoff distance (or residual deflection) reaches a maximum point. The maximum point corresponds to the inflexion point standoff. However, it applies only to "thick" plates ($D/t \leq 70$).
- This maximal dynamic springback corresponds to a gradual shift between a dominant elastic and plastic structural response. Here again, it applies only to "thick" plates ($D/t \leq 70$).

7. References

[1] Jones N. Impulsive loading of a simply supported circular rigid plastic plate. ASME J Appl Mech 1968:59-65.

[2] Gupta AD, Gregory FH, Bitting RL, Bhattacharya S. Dynamic analysis of an explosively loaded hinged rectangular plate. J Computers & Structures 1987;26:339-344.

[3] Jones N, Uran TO, Tekin SA, The dynamic plastic behaviour of fully clamped rectangular plates. Int J Solids Struct 1970;6:1499-512.

[4] Nurick GN, Martin JB. Deformation of thin plates subjected to impulsive loading – a review: Part I – Theoretical studies, Part II – Experimental studies. Int J Impact Eng 1989; 8(2):159-86.

[5] Jones N. Structural impact. Cambridge University Press, 1989.

[6] Teeling-Smith RG, Nurick GN. The deformation and tearing of thin circular plates subjected to impulsive loads. Int J Impact Eng 1991;11:77-91.

[7] Shen WQ, Jones N. Dynamic response and failure of fully clamped circular plates under impulsive loading. Int J Impact Eng 1993;13(2):259-78.

[8] Nurick GN, Olson MD, Fagnan JR, and Levin A. Deformation and tearing of blast-loaded stiffened square plates. Int J Impact Eng 1995; 16(2):273-291.

[9] Nurick GN, Shave GC. The deformation and tearing of thin square plates subjected to impulsive loads-an experimental study. Int J Impact Eng 1996; 18(1):99-116.

[10] Galiev SU. Experimental observations and discussion of counterintuitive behavior of plates and shallow shells subjected to blast loading. Int J Impact Eng 1996; 18(7-8):783-802.

[11] Nurick GN, Gelman ME, and Marshall NS. Tearing of blast loaded plates with clamped boundary conditions. Int J Impact Eng 1996; 18(7-8):803-827.

[12] Harding JE. Response of stiffened and unstiffened plates subjected to blast loading. Engineering Structures 1998; 20(12):1079-1086.

[13] Rudrapantna NS, Vaziri R, and Olson MD. Deformation and failure of blast-loaded square plates. Int J Impact Eng 1999; 22:449-467.

[14] Rudrapantna NS, Vaziri R, and Olson MD. Deformation and failure of blast-loaded stiffened plates. Int J Impact Eng 2000; 24:457-474.

[15] Ramajeyathilagam K, Vendhan CP, and Bhujanga V Rao. Non-linear transient dynamic response of rectangular plates under shock loading. Int J Impact Eng 2000; 24:999-1015.

[16] Chung Kim Yuen S, and Nurick GN. Experimental and numerical studies on the response of quadrangular stiffened plates. Part I: subjected to uniform blast load. Int J Impact Eng 2005;31:55-83.

[17] Langdon GS, Chung Kim Yuen S, and Nurick GN. Experimental and numerical studies on the response of quadrangular stiffened plates. Part II: localised blast loading. Int J Impact Eng 2005;31:85-111.

[18] Hause T, Librescu L. Dynamic response of anisotropic sandwich flat panels to explosive pressure pulses. Int J Impact Eng 2005;31:607-628.

[19] Menkes SB, and Opat HJ, Tearing and shear failure in explosively loaded clamped beams. Exp Mech 1973; 13:480-6.

[20] Chen P, Koç M. Simulation of springback variation in forming of advanced high strength steels. Journal of Materials Processing Technology 2007;190(1-3):189-198.

[21] Zang SL, Liang J, Guo C. A constitutive model for spring-back prediction in which the change of Young's modulus with plastic deformation is considered. Int J of Machine Tools and Manufacture 2007;47(11):1791-1797.

[22] Schleyer GK, Hsu SS, White MD, Birch RS. Pulse pressure loading of clamped mild steel plates. Int J Impact Eng 2003;28(2):223-47.

[23] Neuberger A, Peles S, Rittel D. Scaling the response of circular plates subjected to large and close-range spherical explosions. Part I: air-blast loading. Int. J. Impact Eng 2007; 34(5): 859-873.

[24] LS-DYNA, Livermore Software Technology Corporation. Lawrence Livermore National Laboratory, Livermore, CA, USA.

[25] Kingerly C, and Bulmarsh G. Airblast parameters from TNT spherical air burst and hemispherical surface burst. ARBRL-TR-02555, U.S.Army Ballistic Research Laboratory, Aberdeen Proving Ground, MD, 1984.

[26] CONWEP, Conventional Weapons Effects, US Army TM-855, 1992.

[27] MacNeal-Schwendler Corp. MSC/PATRAN, preprocessing and postprocessing software.

[28] Cowper GR, Symonds PS. Strain hardening and strain rate effect in the impact loading of cantilever beams. Brown Univ. Applied Mathematics Report, 1958: p.28.

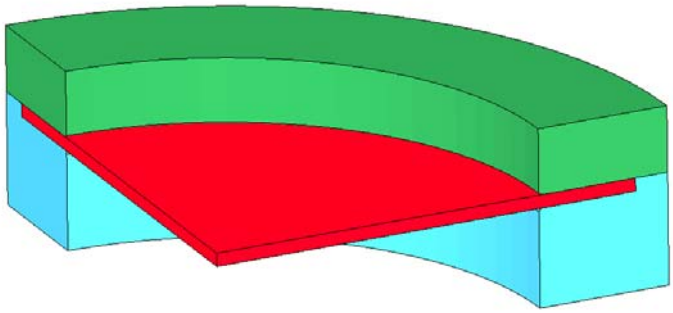

Figure 1: The symmetrical model of quarter of the clamped plate.

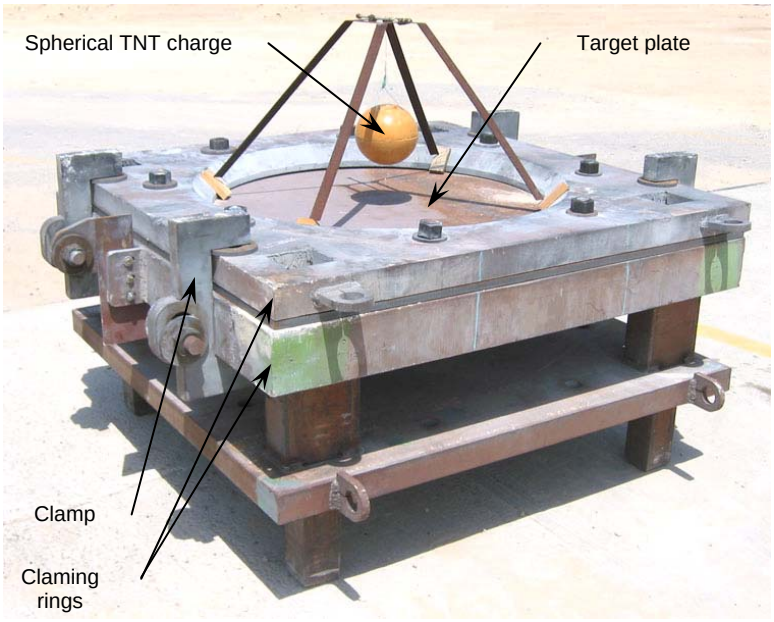

Figure 2: The experimental setup

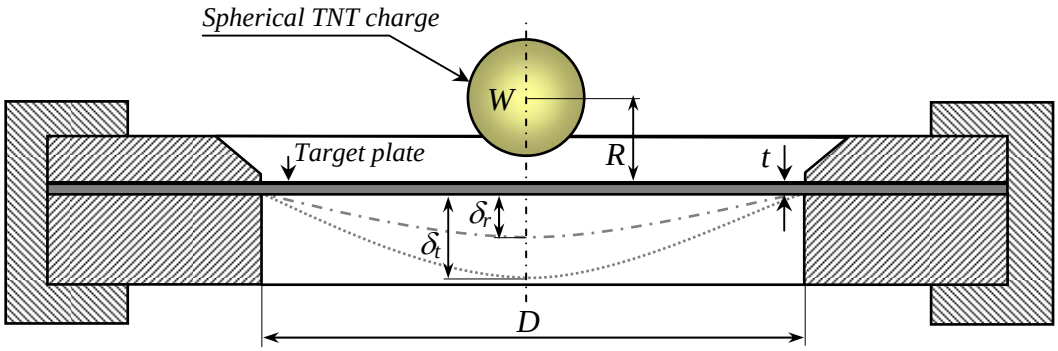

Figure 3: Air blast experimental setup

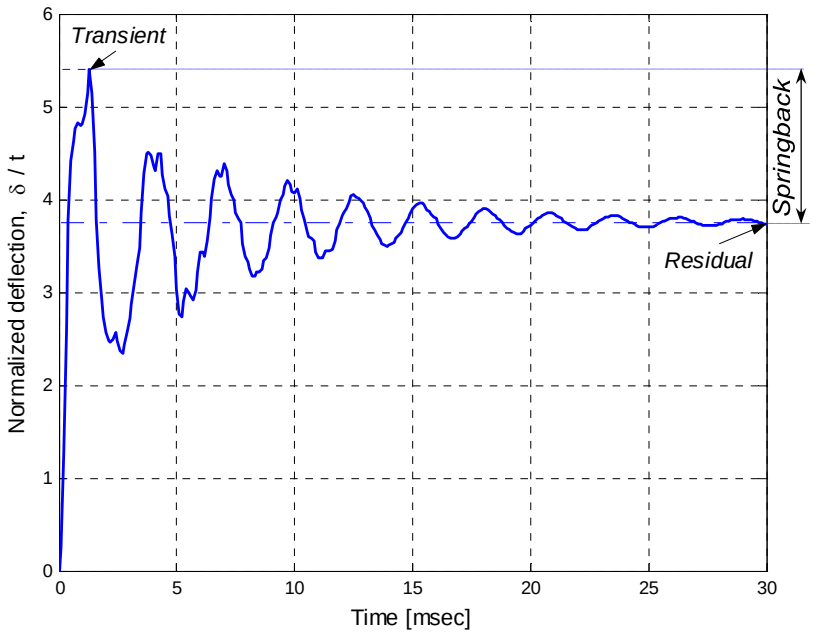

Figure 4: Finite elements results of the mid-point normalized deflection time history of 20mm RHA steel plate after being subjected to 8.75KgTNT from distance of 0.2m.

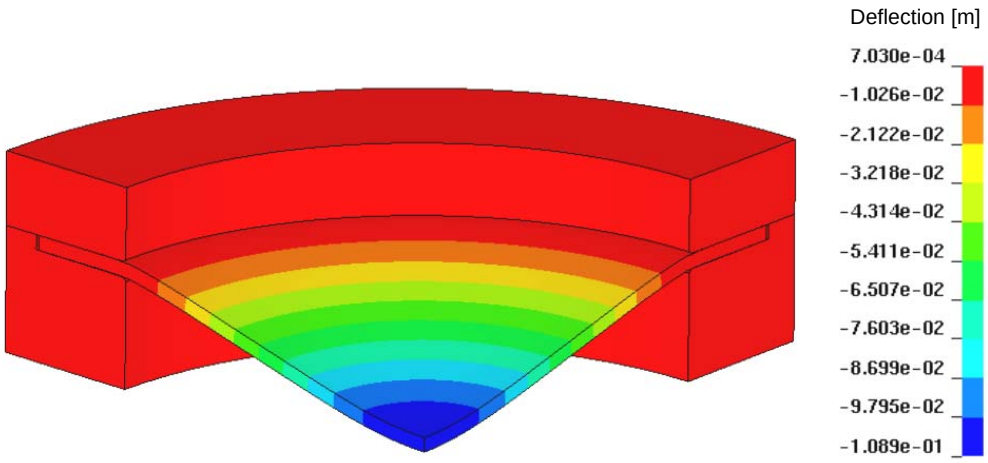

Figure 5: FE 20mm plate subjected to 8.75KgTNT from distance of 0.2m, frame taken close to the transient maximal deflection, after 1.3msec.

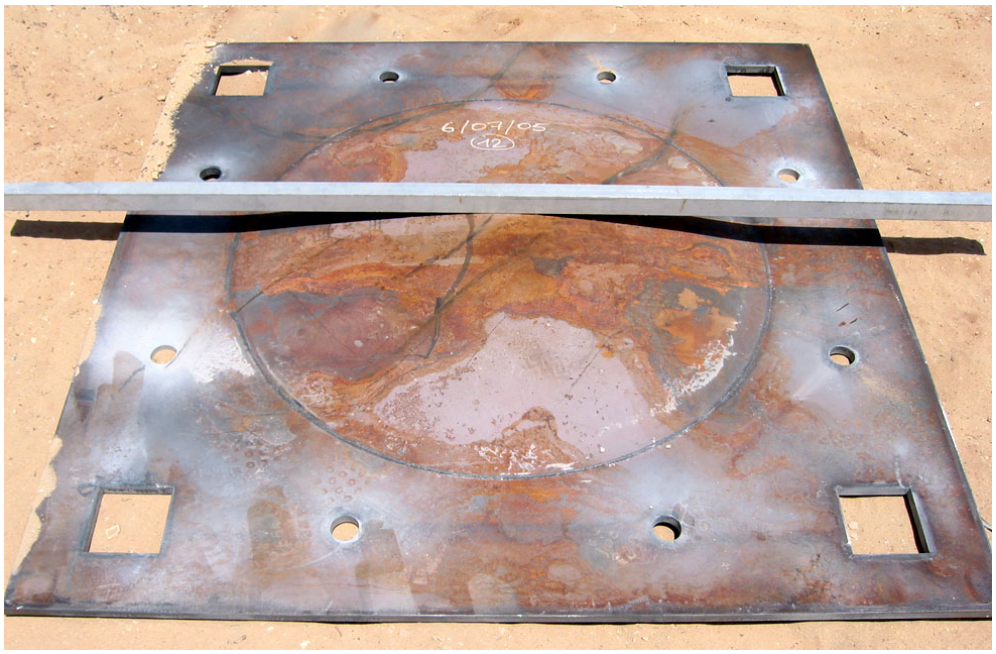

Figure 6: The residual deflection of 20mm RHA steel plate that was subjected to 8.75KgTNT from distance of 0.2m.

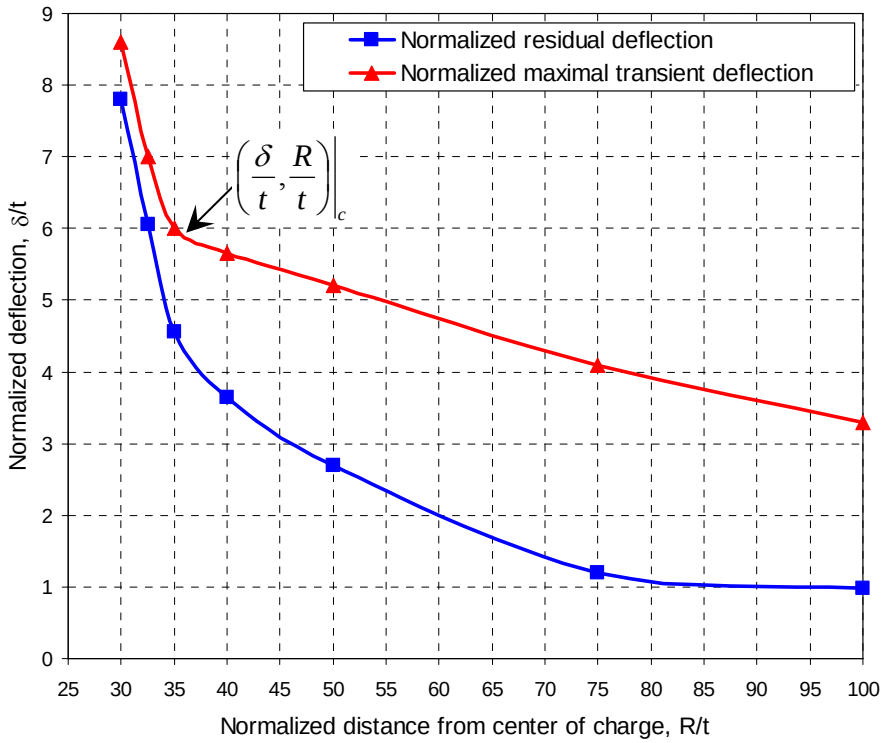

Figure 7: The normalized deflections versus normalized distance from center of charge, for RHA steel plate with scaled thickness t/S=0.01m and D/t=100, subjected to $15S^3$Kg TNT.

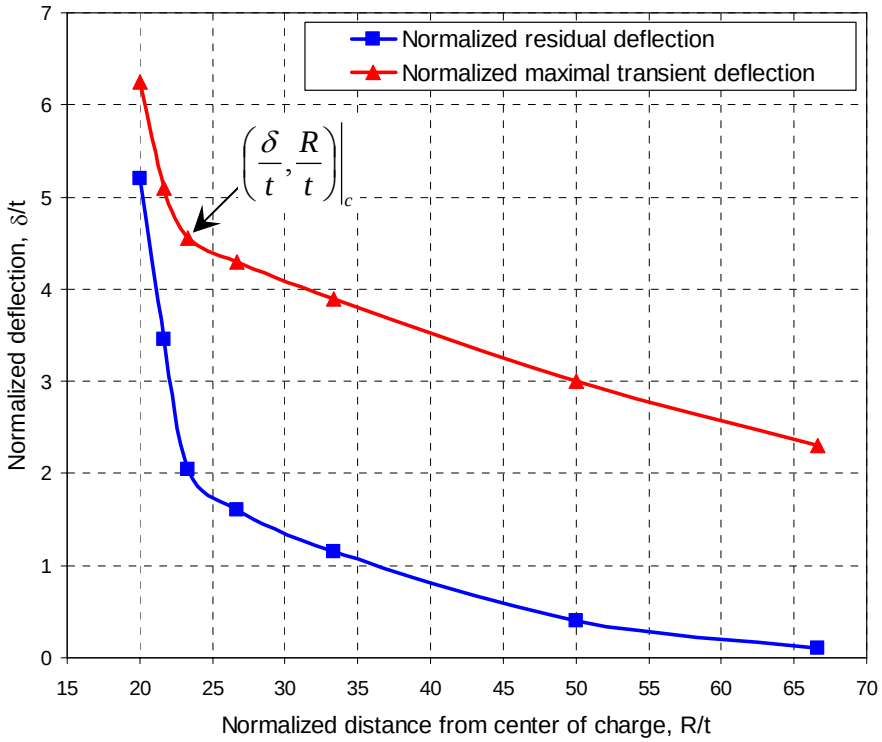

Figure 8: The normalized deflections versus normalized distance from center of charge, for RHA steel plate with scaled thickness t/S=0.015m and D/t=66.67, subjected to 15S^3Kg TNT.

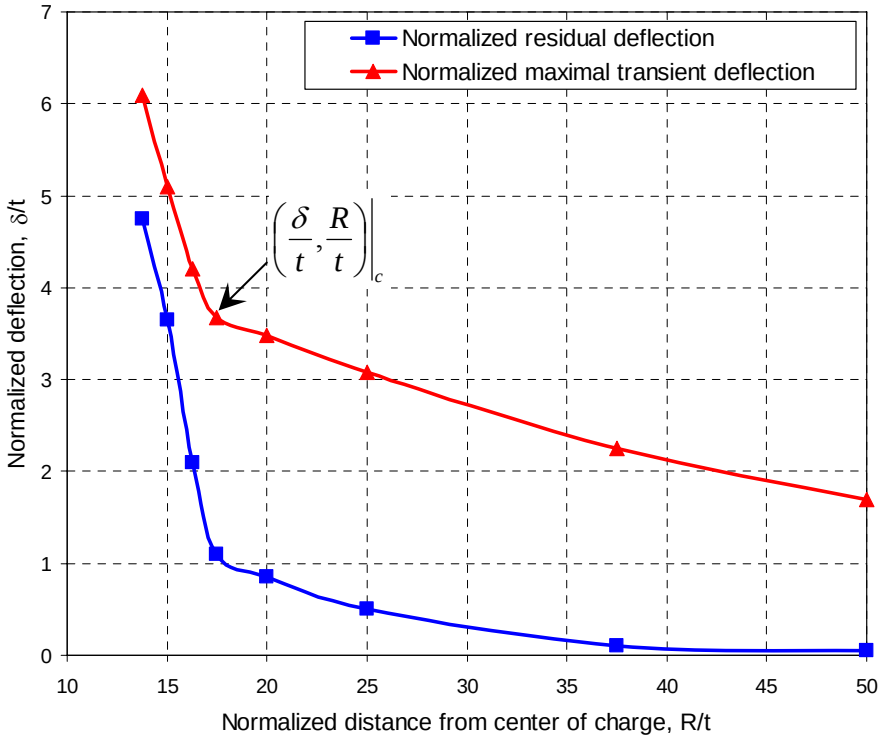

Figure 9: The normalized deflections versus normalized distance from center of charge, for RHA steel plate with scaled thickness t/S=0.02m and D/t=50, subjected to 15S^3Kg TNT.

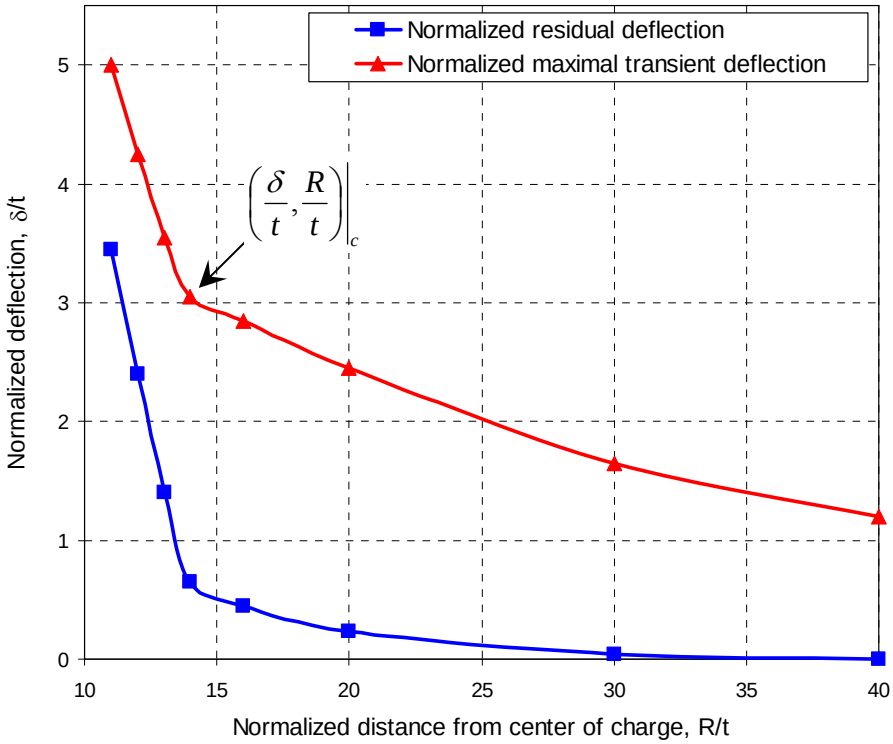

Figure 10: The normalized deflections versus normalized distance from center of charge, for RHA steel plate with scaled thickness t/S=0.025m and D/t=40, subjected to $15S^3$Kg TNT.

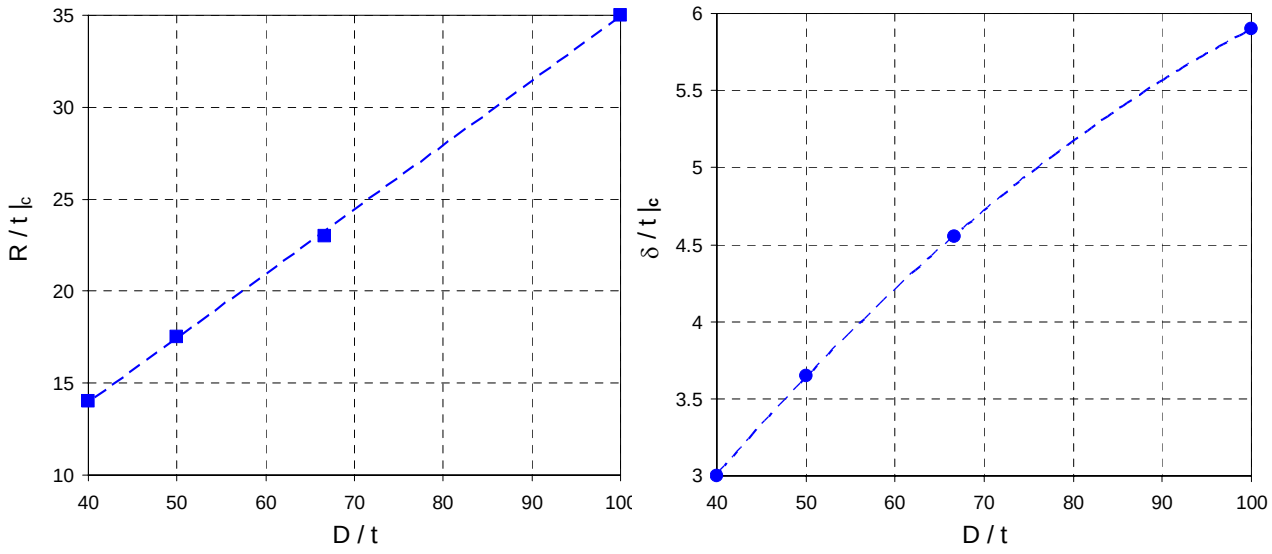

Figure 11: Inflexion point (the non-dimensional distance from charge and non-dimensional transient deflection) versus the plate geometrical characteristics (diameter to thickness ratio).

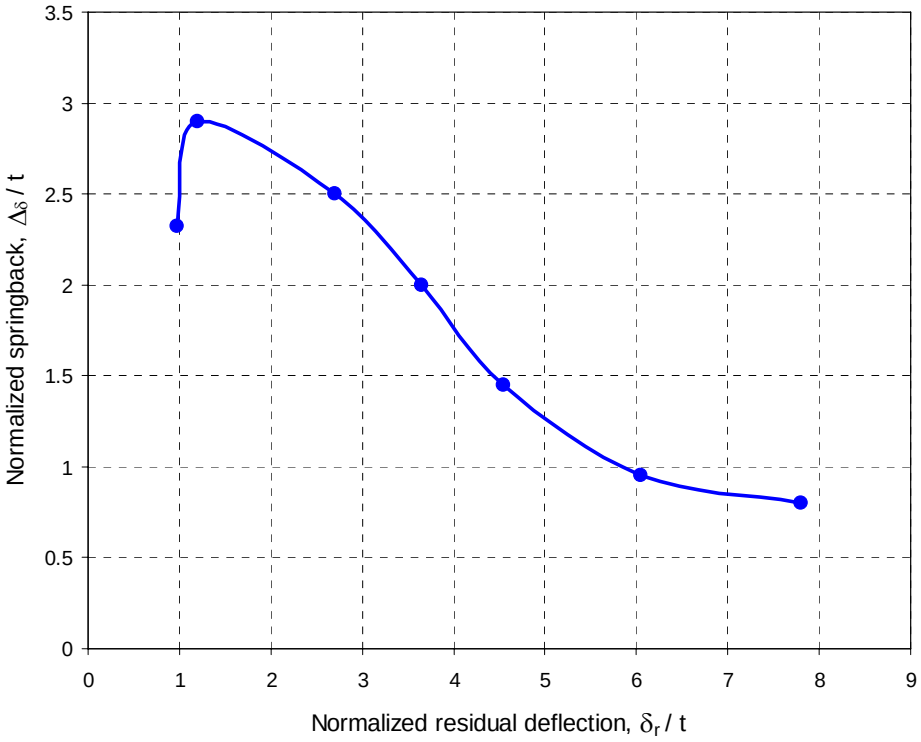

Figure 12: Normalized springback versus normalized residual deflection for RHA steel plate with scaled thickness of t/S=0.01m and D/t=100, subjected to scaled spherical charge of $15S^3$Kg TNT.

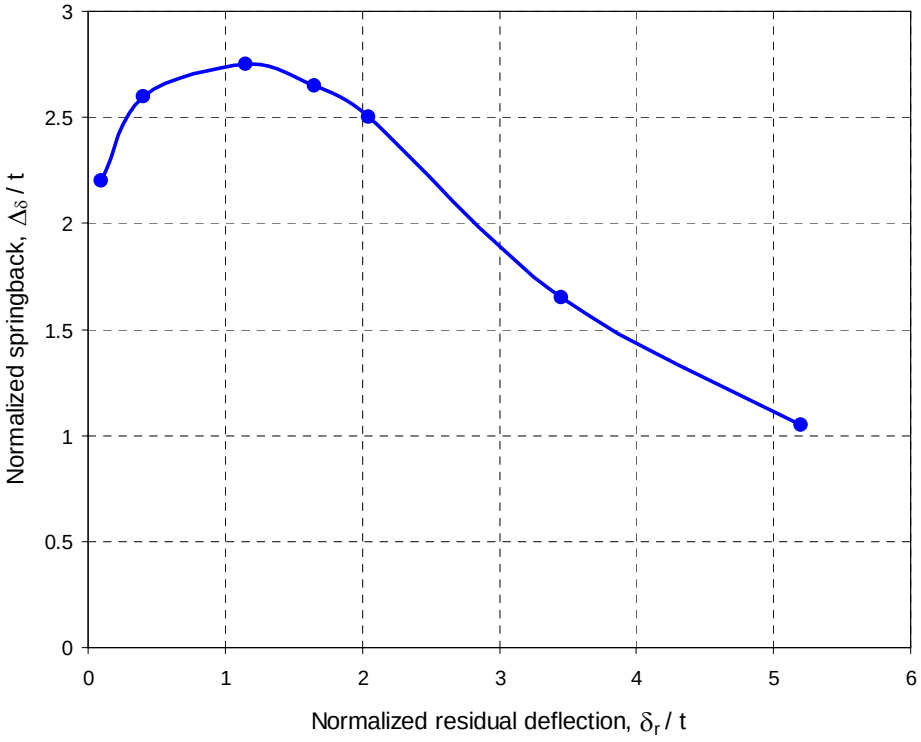

Figure 13: Normalized springback versus normalized residual deflection for RHA steel plate with scaled thickness of t/S=0.015m and D/t=66.67, subjected to scaled spherical charge of $15S^3$Kg TNT.

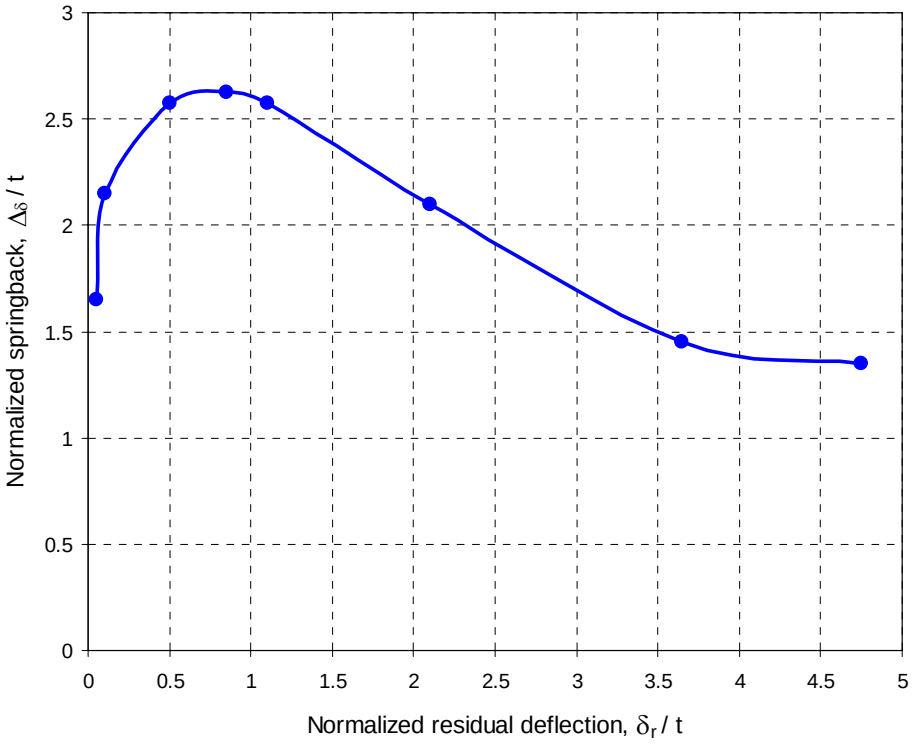

Figure 14: Normalized springback versus normalized residual deflection for RHA steel plate with scaled thickness of t/S=0.02m and D/t=50, subjected to scaled spherical charge of $15S^3$Kg TNT.

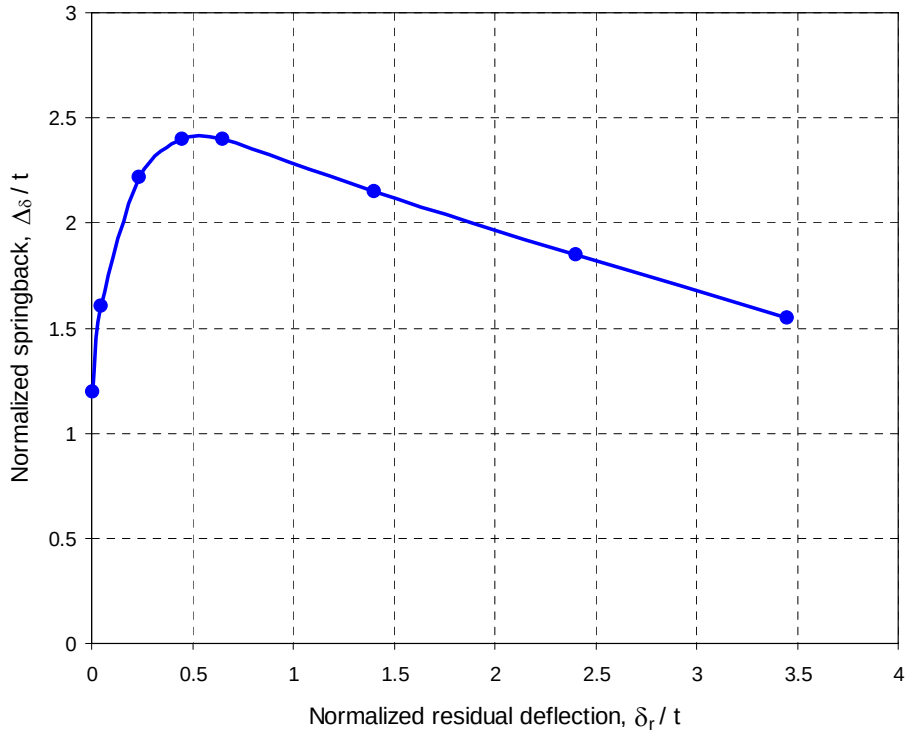

Figure 15: Normalized springback versus normalized residual deflection for RHA steel plate with scaled thickness of t/S=0.025m and D/t=40, subjected to scaled spherical charge of $15S^3$Kg TNT.

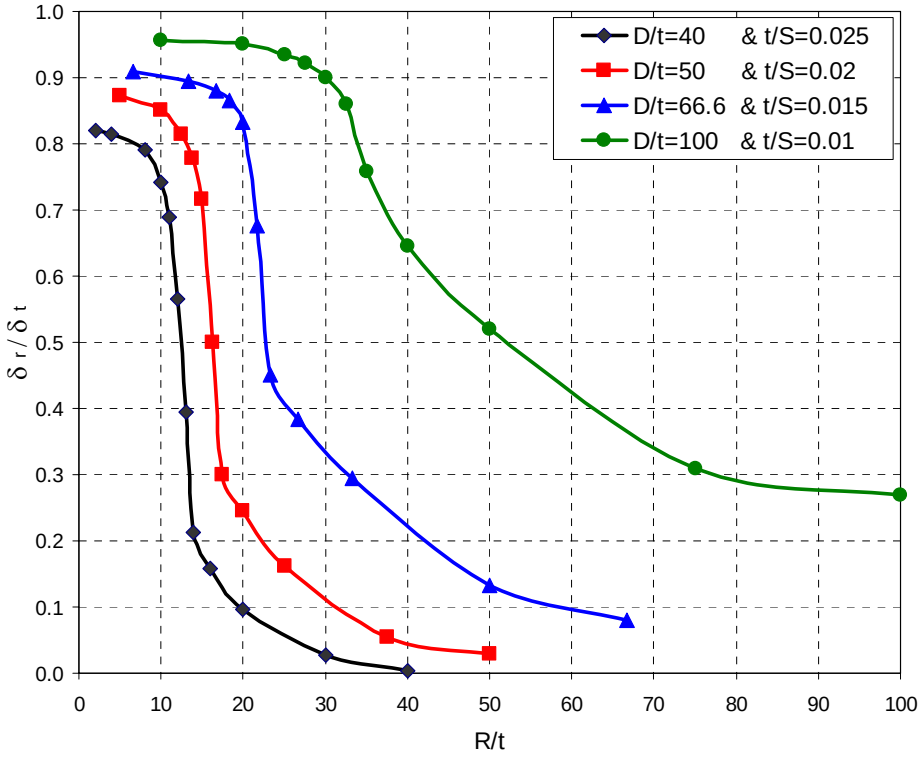

Figure 16: Residual to transient (max.) deflections ratio versus normalized distance from charge for different RHA steel plate diameter to thickness ratios that are subjected to $15S^3$Kg TNT scaled charge.

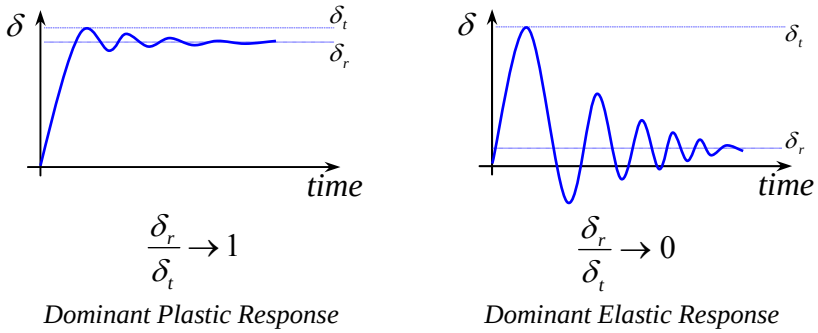

Figure 17: Dominant elastic and plastic response